Production and Infrared Absorption Spectrum of $ClSO_2$ in Matrices†

Mohammed Bahou, Shih-Fung Chen, and Yuan-Pern Lee*

Department of Chemistry, National Tsing Hua University, 101, Sec. 2, Kuang Fu Road, Hsinchu, Taiwan 30013

Received: October 26, 1999; In Final Form: January 31, 2000

A new species, $ClSO_2$, is produced and identified with infrared (IR) absorption spectra when an argon or krypton matrix containing Cl_2 and SO_2 is irradiated with laser emission at 355 nm. Lines at 1311.0, 1309.6, 1099.8, 1098.2, 497.7, and 455.8 cm^{-1} (or 1309.5, 1098.5, 497.0, and 454.2 cm^{-1}) are assigned to $ClSO_2$ isolated in solid Ar (or Kr). Assignments of IR absorption lines are based on results of ^{34}S and ^{18}O isotopic substitution (in solid Kr) and theoretical calculations. Theoretical calculations using density-functional theories (B3LYP and B3P86 with an aug-cc-pVTZ basis set) were performed to predict the geometry, energy, vibrational frequencies, and infrared intensities of possible isomers of $ClSO_2$: (pyramidal) $ClSO_2$, *cis*-ClOSO, (nonplanar) ClOSO, and *cis*-ClSOO. Results predicted for pyramidal $ClSO_2$ agree with observed experimental data. This is the first identification of $ClSO_2$, which is presumably an important intermediate during photolysis of Cl_2SO_2 and in the reaction of Cl with SO_2, especially at low temperatures. In addition to $ClSO_2$, irradiation of the $Cl_2/SO_2/Ar$ matrix sample with laser light at 308 nm produces Cl_2SO_2. Possible mechanisms of formation are discussed.

I. Introduction

The reaction of Cl with SO_2

$$Cl + SO_2 \xrightarrow{M} \text{products} \qquad (1)$$

may play an important role in coupling of chlorine and sulfur cycles in the atmosphere. Kaufman and co-workers[1,2] reported the only kinetic investigation of this reaction; small termolecular rate coefficients, $k_1 = (2.2 \pm 1.8) \times 10^{-34} \exp[(1240 \pm 1050)/RT]$ and $(9.9 \pm 8.1) \times 10^{-34} \exp[(1770 \pm 970)/RT]$ cm^6 $molecule^{-2}$ s^{-1} with Ar and SO_2, respectively, as third bodies were determined with a fast-flow reactor coupled with a modulated molecular-beam mass spectrometer. Although such values of k_1 imply that reaction 1 is probably unimportant in linking chlorine and sulfur cycles in the terrestrial stratosphere, a possibility remains that reaction 1 may be important in the vicinity of a volcanic eruption or in the atmosphere of Venus in which sulfur compounds are present at large concentrations.[3] DeMore et al.[3] employed a Fourier transform infrared (FTIR) spectroscopy to find that SO_2 is quantitatively converted to sulfuryl chloride (Cl_2SO_2) during photolysis of a mixture containing Cl_2 and SO_2. With their modified model for the stratospheric chemistry of Venus, it appears that Cl_2SO_2 is a key reservoir species for chlorine and that reaction 1 contributes to an important cycle for destroying O_2 and converting SO_2 to H_2SO_4.

Li[4,5] performed ab initio calculations on XSO and XSO_2 (X = F, Cl) in their electronic ground and first excited states with Møller−Plesset perturbation theory with second-order correction of correlation energy (MP2) and with quadratic configuration interaction including single and double substitution (QCISD) to predict geometry, energy, vibrational frequencies, and IR intensities of these species. They found that $ClSO_2$ is nonplanar with S at the top of the pyramid; the Cl−S bond distance (2.13−2.15 Å) is relatively large. There seems to exist no experimental report of $ClSO_2$, even though it might be an important intermediate during photolysis of Cl_2SO_2 and in reaction of Cl with SO_2.

We have demonstrated the advantages of matrix isolation as a technique in producing novel isomeric species by making use of selective laser photolysis and matrix cage effect.[6−13] In this paper, we report production and identification of $ClSO_2$ in matrices with infrared spectra according to such techniques, and quantum-chemical calculations of possible isomers of $ClSO_2$.

II. Experiments

The experimental setup is similar to one described previously.[6,10] Matrix samples were prepared on co-depositing mixtures of Cl_2/R_g and SO_2/R_g (R_g = Ar or Kr) with a typical volumetric ratio of $Cl_2/SO_2/R_g \simeq 2/1/400$ onto a platinum-plated copper mirror maintained at 13 K. Approximately 4−10 mmol of mixture was deposited over a period of 3 h.

A XeCl excimer laser (308 nm, 10 Hz with energies ∼5 mJ/pulse) and a frequency-tripled Nd:YAG laser (355 nm, 10 Hz, ∼5 mJ/pulse) were employed to photodissociate Cl_2 to facilitate the reaction of Cl + SO_2. Dye lasers (pumped by a XeCl excimer laser or a frequency-doubled Nd:YAG laser) were used to perform secondary photolysis at 415 and 640 nm. IR absorption spectra were recorded after each stage of photoirradiation with an FTIR spectrometer equipped with a KBr beam splitter and a Hg−Cd−Te detector (77 K). For the far-infrared region, a Mylar beam splitter and a pyroelectric DTGS detector were used. Typically, 900 scans were collected at a resolution of 0.3 cm^{-1}.

SO_2 (99.98%, Matheson), Cl_2 (99.9%, Solkatronic), Ar (99.999%, Spectra Gases), and Kr (99.995%, Scientific Gas Products) were used without further purification except degas-

* To whom correspondence should be addressed. Jointly appointed by the Institute of Atomic and Molecular Sciences, Academia Sinica, Taipei, Taiwan. E-mail: yplee@chem.nthu.edu.tw. Fax: 886-3-5722892.

† Part of the special issue "Marilyn Jacox Festschrift".

10.1021/jp993792w CCC: $19.00
Published on Web 03/17/2000

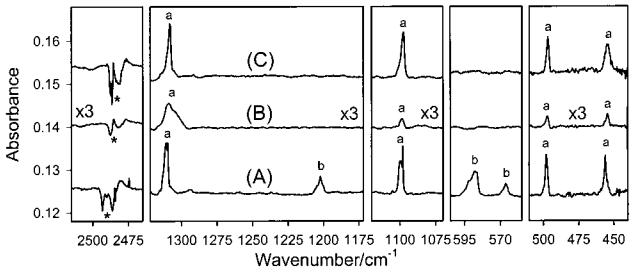

Figure 1. Difference spectra of $Cl_2/SO_2/R_g$ (2/1/400) matrix samples after irradiation: (A) R_g = Ar, irradiation at 308 nm for 20 min; (B) R_g = Kr, irradiation at 355 nm for 20 min; (C) after annealing of the matrix described in (B) at 20 K for 3 min.

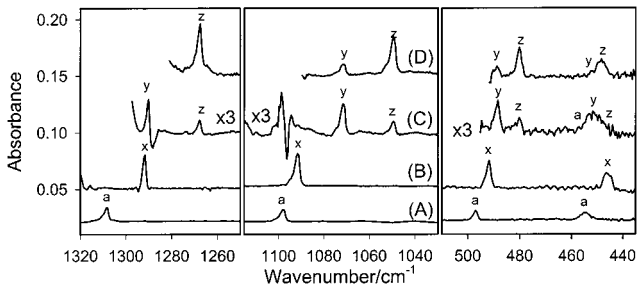

Figure 2. Difference spectra of various isotopically labeled Cl_2/SO_2/Kr matrix samples after irradiation at 355 nm for 20 min: (A) SO_2; (B) $^{34}SO_2$; (C) scrambled ^{16}O- and ^{18}O-substituted SO_2, ^{16}O:$^{18}O \simeq 1:1$; (D) scrambled ^{16}O- and ^{18}O-substituted SO_2, ^{16}O:$^{18}O \simeq 1:6$.

sing of SO_2 and Cl_2 at 77 K. $^{34}SO_2$ and $S^{18}O_2$ (Cambridge Isotope Laboratories) have nominal isotopic purity of 93.5% and 90%, respectively.

III. Computational Method

The equilibrium structure, vibrational frequencies, IR intensities, and single point energies were calculated with the Gaussian 98 program.[14] We used three methods: MP2[15] and density functional theory (DFT) of two types, B3LYP and B3P86. The B3LYP method uses Becke's three-parameter hybrid exchange functional, which includes the Slater exchange functional with corrections involving a gradient of the density, and a correlation functional of Lee, Yang, and Parr, with both local and nonlocal terms.[16,17] The B3P86 method uses Becke's three-parameter hybrid exchange functional with Perdew's gradient-corrected correlation functional.[18,19] The standard 6-31+G* basis set were used in MP2 calculations and Dunning's correlation-consistent polarized valence triplet-zeta basis set, augmented with s, p, d, and f functions (aug-cc-pVTZ)[20] were applied in DFT calculations. Analytic first derivatives were utilized in geometry optimization, and vibrational frequencies were calculated analytically at each stationary point.

IV. Results and Discussion

A. Production of $ClSO_2$. The IR spectra of SO_2 in various matrices are well characterized.[11,21−23] Our observation of SO_2 lines at 1355.2, 1351.1, 1152.2, 1147.1, 519.7, and 517.3 cm^{-1} (in solid Ar) and 1350.9, 1149.8, and 519.0 cm^{-1} (in solid Kr) are consistent with previous reports. An additional set of lines at 1348.2, 1146.6, and 516.7 cm^{-1} were observed for SO_2 in solid Kr at concentrations $SO_2/Kr \simeq 1/200$. Although absorption lines of Cl_2 at 549.2 and 554.3 cm^{-1} (in solid Ar)[24] and at 547.1 cm^{-1} (in solid Ar, due to perturbation by O_3)[25] are reported, we observed no such absorption in our Cl_2/SO_2/Ar (Kr) matrix.

Irradiation of an Ar matrix sample containing Cl_2 and SO_2 with laser emission at 308 nm for 20 min produced lines in two sets at 1309.6, 1098.2, 497.7, and 455.8 cm^{-1} (marked "a"), and at 1425.3, 1202.3, 586.3, and 566.5 cm^{-1} (marked "b"), as shown in the difference spectrum Figure 1A. Additional broad lines at 1311.6 and 1099.8 cm^{-1} in set "a" are observed; they are due to matrix site splitting. Because the fundamental lines of SO_2 are saturated, weak lines due to $\nu_1 + \nu_3$ combination near 2480 cm^{-1} (Figure 1) are used to monitor the variation in concentration of SO_2. Irradiation of a Kr matrix sample containing Cl_2 and SO_2 with laser emission at 355 nm produced similarly four lines at 1309.5, 1098.5, 497.0, and 454.2 cm^{-1}, as shown in Figure 1B. Lines corresponding to those marked "b" in Figure 1A are not produced at this photolysis wavelength. Annealing of the irradiated sample at 20 K for 3 min followed by cooling to 13 K enhanced the intensities of these lines, as shown in Figure 1C. As intensities of new lines (set "a") increase after annealing, the intensity of the $\nu_1 + \nu_3$ line of SO_2 decreases, indicating that these new lines may be associated with a species produced on reaction of Cl with SO_2. Lines at 1309.5, 1098.5, and 497.0 cm^{-1} (in Kr) are close to those of SO_2 (1350.9, 1149.5, and 519.0 cm^{-1}), indicating that the new species may contain a SO_2 moiety. Observation of a fourth line at 454.4 cm^{-1} indicates that the species contains more than three atoms.

Lines in set "b" observed after photolysis of the matrix sample at 308 nm are readily assigned to absorption of Cl_2SO_2. Literature values for IR absorption of gaseous Cl_2SO_2 are 1434, 1205, 586, and 577 cm^{-1} (ref 26), or 1437 and 1212 cm^{-1} (ref 3). We also recorded an IR absorption spectrum of Cl_2SO_2 isolated in solid Ar (Cl_2SO_2/Ar = 1/1700) and observed lines at 1425.9, 1200.5, 585.6, and 564.8 cm^{-1}, consistent with observed values for set "b".

A far-IR spectrum of the irradiated matrix sample was also recorded in the spectral region 200−700 cm^{-1}; no new line other than those already detected at 497.0 and 454.2 cm^{-1} was observed.

B. ^{34}S and ^{18}O Isotopic Experiments. Because there are multiple matrix sites for the new species (set "a") in solid Ar, we perform isotopic experiments in a Kr matrix in order to avoid interference due to site splitting.

Similar experiments with photolysis of a $Cl_2/^{34}S^{16}O_2$/Kr (2/1/400) matrix sample at 355 nm yield lines at 1291.6, 1091.4, 491.8, and 445.6 cm^{-1} (marked "x"), as shown in Figure 2B. A spectrum recorded after photolysis of the $Cl_2/^{32}S^{16}O_2$/Kr sample is shown in Figure 2A for comparison. When $^{32}S^{16}O_2$ was replaced with a scrambled mixture of $^{32}SO_2$ with ^{16}O:$^{18}O \simeq 1:1$, the resultant spectrum (Figure 2C) recorded after irradiation at 355 nm shows two additional lines (marked "y" and "z") for each of the three high-frequency lines in Figure 2A; loss of the reactant isotopomer $S^{18}O_2$ interferes with lines associated with natural isotopomer of the new species. Isotopic lines near 452 cm^{-1} are unresolved; the broadened line width is ~6.2 cm^{-1}. To investigate further this broad feature, we employed a second scrambled mixture of SO_2 with a ratio ^{16}O:$^{18}O \simeq 1:6$; the resultant spectrum is shown in Figure 2D. In this case the line at 448.4 cm^{-1} exhibits a line width similar to the corresponding member at 454.2 cm^{-1} (from the $Cl_2/S^{16}O_2$/Kr sample) with wavenumber decreased by 5.8 cm^{-1}. The broad feature in Figure 2C is thus deconvoluted into three lines with two lines fixed at 454.2 and 448.4 cm^{-1} to yield the peak position of the central line at 452.4 ± 0.3 cm^{-1}. Wavenumbers of observed new lines that are associated with each isotopic species are listed in Table 1.

Upon ^{34}S substitution, the four lines shift toward smaller wavenumbers by 17.9, 7.1, 5.2, and 8.6 cm^{-1}, respectively, indicating that all four modes involve the motion of the S atom.

TABLE 1: Observed Vibrational Wavenumbers/cm^{-1} of Various Isotopic Species of $ClSO_2$ Isolated in Matrices

	$ClSO_2$		$Cl^{34}SO_2$	$ClS(^{16}O)^{18}O$	$ClS^{18}O_2$
mode	in Ar	in Kr	in Kr	in Kr	in Kr
ν_1	1309.6 (1311.0)[a]	1309.5	1291.6	1290.6	1267.6
ν_2	1098.2 (1099.8)[a]	1098.5	1091.4	1071.6	1049.5
ν_3	497.7	497.0	491.8	488.8	480.1
ν_4	455.8	454.2[b]	445.6	~452.4[c]	448.4

[a] Broad features. [b] This feature is deconvoluted to two lines at 455.3 and 453.4 cm^{-1}, corresponding to $^{35}ClSO_2$ and $^{37}ClSO_2$, respectively; see text. [c] Deconvoluted from a broad feature containing $ClS^{16}O_2$, $ClS(^{16}O)^{18}O$, and $ClS^{18}O_2$; see text.

Two high-frequency lines at 1309.5 and 1098.5 cm^{-1} shift substantially (41.9 and 49.0 cm^{-1}) upon ^{18}O substitution (Figure 2D). The isotopic ratios (defined as ratio of wavenumber of a specific isotopomer to that of the natural species) of the fully ^{18}O-substituted species, 1267.6/1309.5 = 0.9680 and 1049.5/1098.5 = 0.9554 for lines at 1309.5 and 1098.5 cm^{-1}, respectively, are similar to ratios 0.9680 and 0.9560 for asymmetric stretching (ν_3) and symmetric stretching (ν_1) modes of $S^{18}O_2$ (Table 4 of ref 11). A single component for the central line of the triplet that was observed for scrambled ^{18}O and ^{16}O species (Figure 2C) indicates that motion of two O atoms is equivalent in these modes. The isotopic ratios of 1290.6/1309.5 = 0.9856 and 1071.6/1098.5 = 0.9755 for lines at 1309.5 and 1098.5 cm^{-1}, respectively, are similar to the ratios 0.9860 and 0.9760 for corresponding modes (ν_3 and ν_1) of $^{16}OS^{18}O$. Hence lines at 1309.5 and 1098.5 cm^{-1} are assigned to asymmetric stretching and symmetric stretching modes within the SO_2 moiety of the new species. The line at 497.0 cm^{-1} is red-shifted by 8.2 and 16.9 cm^{-1} upon ^{18}O substitution. Observed isotopic ratios of 0.9835 and 0.9660 differ slightly from values 0.9790 and 0.9580 for the bending (ν_2) mode of $^{16}OS^{18}O$ and $S^{18}O_2$, respectively (ref 11), indicating a small change of OSO bond angle or mode mixing for this vibration. That only a single component is observed for the central line of the triplet in the scrambled ^{16}O and ^{18}O species indicates that motion of the two O atoms in this mode is equivalent. Hence, the fourth (Cl) atom of this new species must be bonded with the S atom. The ^{18}O isotopic shift (5.8 cm^{-1}) of the line at 454.2 cm^{-1} is smaller than that (8.6 cm^{-1}) for the ^{34}S species, indicating that motion of the S atom is greater than that of O atoms in this mode. As the S atom is likely central, absorption at 454.2 cm^{-1} might be associated with an umbrella motion.

Although the presence of chlorine is required to produce the new species, no observed line shows a distinct pattern of splitting due to ^{35}Cl and ^{37}Cl isotopes. Observed lines are thus not directly associated with the S−Cl stretching mode because ^{37}Cl in natural abundance is expected to yield resolvable line splitting, estimated to be ~6.5 cm^{-1} for a S−Cl stretching mode near 500 cm^{-1}. The observed width (~3.8 cm^{-1}) of the line at 454.2 cm^{-1} is larger than those (~2.4 cm^{-1}) of the other three lines, indicating a small but unresolvable ^{37}Cl shift. After deconvolution of the ν_4 line at 454.2 cm^{-1} with two lines each having a shape similar to those of ν_1−ν_3 and an intensity ratio of 3:1, line positions at 455.3 ± 0.5 and 453.4 ± 0.5 cm^{-1} are derived. The ^{37}Cl isotopic shift ~1.9 cm^{-1} in this mode is consistent with the assignment of an umbrella motion to this line.

On the basis of our experimental results and the consideration that the reaction Cl + SO_2 takes place upon photolysis as well as after annealing, we tentatively assign observed new lines (set "a") to absorption of $ClSO_2$. As shown in the following section, theoretical calculations provide further support of such an assignment.

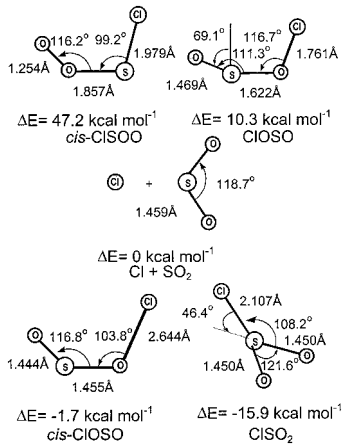

Figure 3. Geometries of four isomers of $ClSO_2$ calculated with the B3P86/aug-cc-pVTZ method.

C. Theoretical Calculations. *1. Geometry and Energy*. According to theoretical calculations (B3LYP and B3P86 with an aug-cc-pVTZ basis set), there are four stable isomers of $ClSO_2$, as illustrated in Figure 3. Predicted geometry and energies of each isomer are listed in Table 2 and compared with previous results on pyramidal $ClSO_2$ using MP2/6-311G(2d) and QCISD/6-31G* methods.[4,5]

The species of the least energy has a pyramidal structure with the S atom on top (designated as $ClSO_2$); it is bound by −10.6 (B3LYP) or −15.9 kcal mol^{-1} (B3P86) compared with Cl + SO_2. A planar cis isomer (designated *cis*-ClOSO) is predicted to lie ~9.2 and 14.2 kcal mol^{-1} above $ClSO_2$ based on B3LYP and B3P86 methods, respectively. It is slightly lower in energy than Cl + SO_2; thus it might be formed after photolysis of the matrix. *cis*-ClOSO has a relatively elongated Cl−O bond; hence it can be taken as a Cl atom loosely attached to the O atom of SO_2. However, the B3P86 method also predicts a second conformer with a nonplanar geometry having a dihedral angle of 69.1° (designated ClOSO), similar to that predicted by the MP2/6-31+G* method. The nonplanar ClOSO has a terminal S═O bond length (1.469 Å) similar to that of SO_2 and a central S−O bond length (1.622 Å) similar to that (~1.62 Å) of SOO.[11] The Cl−O bond length of 1.761 Å is similar to that for ClOOCl (~1.74 Å).[27,28]

A fourth isomer (*cis*-ClSOO) is planar with an elongated S−O bond (1.860 Å) and a short O−O bond (1.254 Å); it lies ~50 kcal mol^{-1} above $ClSO_2$. *cis*-ClSOO is unlikely to be produced in our experiment as reaction from Cl + SO_2 involves rearrangement of O atoms and is endothermic by ~50 kcal mol^{-1}. Similarly, ClOSO is unlikely to be produced in the matrix.

The geometry of $ClSO_2$ predicted with various theoretical methods is consistent except for the length of the Cl−S bond. Both B3LYP and QCISD methods predict a Cl−S bond ~2.150 Å, whereas the B3P86 method yields 2.107 Å. The SO_2 moiety in $ClSO_2$ resembles SO_2 itself, with nearly identical bond length but a greater bond angle ~121.5°, compared with 118.7° for SO_2.

2. Vibrational Wavenumbers and Mode Assignments. Vibrational wavenumbers and infrared intensities of four isomers of $ClSO_2$ predicted with various theoretical methods are listed in Table 3. For pyramidal $ClSO_2$, variations in wavenumbers for lines above 400 cm^{-1} among QCISD, B3LYP, and B3P86 methods are within 8.7% with an average of 3.9 ± 2.8%. Observed wavenumbers of the new species fit well with those predicted for $ClSO_2$, with maximum and averaged deviations

TABLE 2: Geometry and Energies of Four Isomers of $ClSO_2$ Predicted with Various Theoretical Methods

species	parameters	MP2[a]/ 6-31+G*	QCISD[b]/ 6-31G*	B3LYP[a]/ aug-cc-pVTZ	B3P86[a]/ aug-cc-pVTZ
$Cl + SO_2$	E/hartree	−1007.252477		−1008.878761	−1009.775300
$ClSO_2$	r_{ClS}/Å	2.118	2.149	2.150	2.107
	r_{SO}/Å	1.468	1.465	1.456	1.450
	∠ClSO (deg)	108.38	107.8	108.30	108.23
	∠OSO (deg)	123.40	122.4	121.35	121.59
	Cl−S off-plane angle	43.80	46.0	46.65	46.43
	E/hartree	−1007.241724	−1007.23965[c]	−1008.895590	−1009.800674
	ΔE[d]/kcal mol^{-1}	6.8		−10.6	−15.9
cis-ClOSO	r_{ClO}/Å			2.740	2.644
	r_{OS}/Å			1.459	1.455
	r_{SO}/Å			1.449	1.444
	∠ClOS (deg)			108.23	103.76
	∠OSO (deg)			117.10	116.81
	dihedral angle (deg)			180.0	180.0
	E/hartree			−1008.881057	−1009.777992
	ΔE[d]/kcal mol^{-1}			−1.4	−1.7
ClOSO	r_{ClO}/Å	1.728			1.761
	r_{OS}/Å	1.711			1.622
	r_{SO}/Å	1.465			1.469
	∠ClOS (deg)	114.25			116.69
	∠OSO (deg)	112.97			111.28
	dihedral angle (deg)	42.15°			69.11°
	E/hartree	−1007.208201			−1009.758839
	ΔE[d]/kcal mol^{-1}	27.8			10.3
cis-ClSOO	r_{ClS}/Å	2.024		2.000	1.979
	r_{SO}/Å	1.738		1.884	1.857
	r_{OO}/Å	1.327		1.262	1.254
	∠ClSO	100.77°		99.59°	99.17°
	∠SOO	112.79°		116.38°	116.16°
	dihedral angle	82.55°		−0.01°	−0.27°
	E/hartree	−1007.131244		−1008.798979	−1009.700115
	ΔE[d]/kcal mol^{-1}	76.1		50.1	47.2

[a] This work. [b] References 4 and 5. The MP2/6-311G(2d) calculations on $ClSO_2$ were also reported. [c] (E + 1007)/hartree = −0.63060 from MP4SDTQ/6-311G(2df, 2pd), −0.63432 from PMP4SDTQ (2df, 2pd), −0.58291 from QSISD/6-311G(2df, 2pd); see refs 4 and 5. [d] Relative to the energy of $Cl + SO_2$.

−4.3% and −2.5 ± 1.2% for the B3LYP method, and 0.9% and 0.3 ± 0.5% for the B3P86 method, respectively. Calculated relative IR intensities also agree satisfactorily with experimental observations, as listed in parentheses in Table 3. IR intensities predicted for two low-frequency modes (ν_5 and ν_6) are at most one-tenth that of the weakest line (454.2 cm^{-1}) observed in this work, consistent with our lack of observation of absorption line of $ClSO_2$ below 400 cm^{-1}.

Wavenumbers predicted for ClOSO (either in a cis planar or a nonplanar form) disagree with those of lines observed in this work. For *cis*-ClOSO, predicted wavenumbers of three vibrational modes of the SO_2 moiety are similar to those predicted for $ClSO_2$, but the relative intensities differ greatly. Our results do not match those predicted for *cis*-ClOSO. For the nonplanar form, the central S−O bond is weak and has a vibrational wavenumber ∼660 cm^{-1}. We searched carefully but failed to locate weak features that might fit with predicted absorption lines of ClOSO or *cis*-ClSOO.

Displacement vector diagrams of each vibrational mode of $ClSO_2$ calculated with the B3P86 method are illustrated in Figure 4. For convenience, modes are numbered according to vibrational wavenumbers rather than symmetry. A side-view and a top-view diagram placed below each of the three-dimensional diagram help to illustrate the motion of each atom. On the basis of predicted displacement vectors, $\nu_1-\nu_3$ are readily assigned to modes for asymmetric stretching, symmetric stretching, and bending motions of the SO_2 moiety, in agreement with assignments based on experimental results. The ν_4 mode is an umbrella or inversion motion with displacement of S atom being greatest, consistent with the experimental observation that the ^{34}S isotopic shift is greater than the ^{18}O isotopic shift for the line at 454.2 cm^{-1}. The ν_5 mode involves Cl−S stretching motion mixed with SO_2 rocking, whereas the ν_6 mode shows a SO_2-wagging motion with accompanying motion of the Cl atom.

3. ^{34}S, ^{18}O, and ^{37}Cl Isotopic Ratios. Predicted and observed isotopic ratios for ^{34}S-, ^{18}O-, and ^{37}Cl-substituted isotopomers of $ClSO_2$ are listed in Table 4. Isotopic ratios predicted with B3LYP and B3P86 methods are similar; they both agree with experimental observations with maximum deviations of 0.10% and 0.42%, respectively, for $\nu_1-\nu_3$. The largest deviations between experimental values and those predicted with B3LYP and B3P86 methods are 0.32% and 0.45%, respectively, for ν_4. As error in deconvolution of lines due to $ClS(^{16}O)^{18}O$ is likely for this mode, the agreement is satisfactory. A ^{37}Cl isotopic shift of ∼1.3 cm^{-1} predicted for the ν_4 mode is consistent with experimental observation of a line further broadened by ∼1.4 cm^{-1}, as compared with those of $\nu_1-\nu_3$ lines. When the deconvoluted value (455.3 cm^{-1}) is used for $\nu_4(^{35}Cl^{32}S(^{16}O)^{16}O)$, agreements in isotopic ratios are improved, as also listed in Table 4.

Predicted isotopic ratios for ^{34}S-, ^{18}O-, and ^{37}Cl-substituted isotopomers of two conformers of ClOSO and *cis*-ClSOO are listed as Supporting Information; no experimental data are available for comparison. Predicted isotopic ratios clearly eliminate the possibility of observed new lines being assigned to ClOSO or *cis*-ClSOO.

D. Formation Mechanism, Secondary Photolysis, and Atmospheric Implication. At 355 nm, SO_2 cannot be dissociated. Photolysis of Cl_2 at 355 nm produces predominantly $Cl(^2P_{3/2})$, with only 1.6% of $Cl(^2P_{1/2})$.[29] Possibility of exit from

TABLE 3: Vibrational Wavenumbers/cm^{-1} and Infrared Intensities of Four Isomers of $ClSO_2$ Predicted with Various Theoretical Methods

species	ν_i	sym	mode	QCISD[a]/ 6-31G*	B3LYP[b]/ aug-cc-pVTZ	B3P86[b]/ aug-cc-pVTZ	expt Kr	expt Ar
$ClSO_2$	ν_1	a″	SO_2 a-str	1299 (100)[c]	1273.4 (100)[c]	1305.9 (100)[c]	1309.5 (100)[c]	1309.6 (100)[c]
	ν_2	a′	SO_2 s-str	1081 (74)	1085.5 (67)	1108.6 (70)	1098.5 (78)	1098.2 (72)
	ν_3	a′	OSO bend	489 (71)	488.62 (59)	497.28 (80)	497.0 (60)	497.7 (59)
	ν_4	a′	$ClSO_2$ umbrella	420 (69)	434.66 (51)	456.51 (39)	454.2 (45)	456.1 (45)
	ν_5	a′	Cl−S str	247	261.24 (5)	288.15 (3)		
	ν_6	a″	SO_2 wag	214 (11)	248.49 (1)	260.10 (1)		
cis-ClOSO	ν_1	a′	SO_2 a-str		1317.6 (100)[c]	1340.8 (100)[c]		
	ν_2	a′	SO_2 *s*-str		1144.9 (11.2)	1163.7 (12.0)		
	ν_3	a′	OSO bend		516.7 (7.9)	522.1 (8.0)		
	ν_4	a′	mixed Cl−O str		102.4 (4.3)	119.3 (5.4)		
	ν_5	a′	ClOS bend		45.5 (0.2)	58.5 (4.9)		
	ν_6	a″	out-of-plane		41.2 (2.3)	41.9 (2.5)		
ClOSO	ν_1	a′	S═O str			1185.5 (100)[c]		
	ν_2	a′	S−O str			663.2 (42.0)		
	ν_3	a′	OSO bend			445.5 (7.3)		
	ν_4	a′	mixed			378.1 (44.0)		
	ν_5	a′	Cl−O str			210.5 (9.6)		
	ν_6	a″	torsion			92.2 (1.7)		
cis-ClSOO	ν_1	a′	O−O str		1236.1 (100)[c]	1274.6 (100)[c]		
	ν_2	a′	S−O str		589.9 (14.6)	612.2 (15.8)		
	ν_3	a′	SOO bend		509.3 (16.5)	528.6 (17.2)		
	ν_4	a′	mixed		282.6 (15.6)	309.4 (15.8)		
	ν_5	a′	mixed Cl−S str		162.2 (1.8)	170.6 (2.2)		
	ν_6	a″	out-of-plane		104.9 (0.0)	113.9 (0.0)		

[a] Reference 5. [b] This work. [c] Relative infrared intensities are listed in parentheses. IR intensities (in km mol^{-1}) for ν_1 are calculated to be 114.4 and 117.9 for $ClSO_2$, 327.6 and 330.3 for *cis*-ClOSO, 155.3 and 150.9 for *cis*-ClSOO, respectively, with B3LYP and B3P86 methods, and 88.9 for ClOSO with B3P86 method.

a matrix cage remains less than 10^{-6} for excitation wavelength greater than 203 nm; at wavelengths between 177 and 203 nm, a dissociation probability of approximately 2% was reported.[30] Hence, $ClSO_2$ is presumably formed during photolysis via reaction of Cl atom with SO_2 within the same matrix cage. Annealing of the matrix sample also facilitates reaction of Cl with SO_2, resulting in increased yield of $ClSO_2$.

The absence of *cis*-ClOSO suggests that either there is a barrier for Cl atom to attack the terminal O atom or *cis*-ClOSO is unstable. Considering possible errors, the small exothermicity predicted by theory does not guarantee the stability of *cis*-ClOSO. Calculations using the MP2-full/6-31+G* method indicate no barrier for formation of $ClSO_2$ from Cl approaching the central S atom of SO_2 but a barrier ~5 kcal mol^{-1} for formation of *cis*-ClOSO from Cl approaching the terminal O atom of SO_2, consistent with our observation of only $ClSO_2$ as a reaction product.

Photolysis of Cl_2 at 308 nm also produces mainly Cl($^2P_{3/2}$) with only 0.95% of Cl($^2P_{1/2}$).[29] Observation of Cl_2SO_2 at this photolysis wavelength rather than 355 nm is confusing. It indicates that either there is a small barrier for the reaction

$$Cl + ClSO_2 \rightarrow Cl_2SO_2 \qquad (2)$$

or excitation of SO_2 to a long-lived electronically excited triplet state plays a role in the formation of Cl_2SO_2. As annealing of the matrix after irradiation at 355 nm produces no Cl_2SO_2 despite an expectation that Cl and $ClSO_2$ might coexist appreciably within the same matrix cage, a small barrier for reaction 2 is needed to explain why Cl_2SO_2 was observed upon photolysis at 308 nm rather than 355 nm. At smaller photolysis

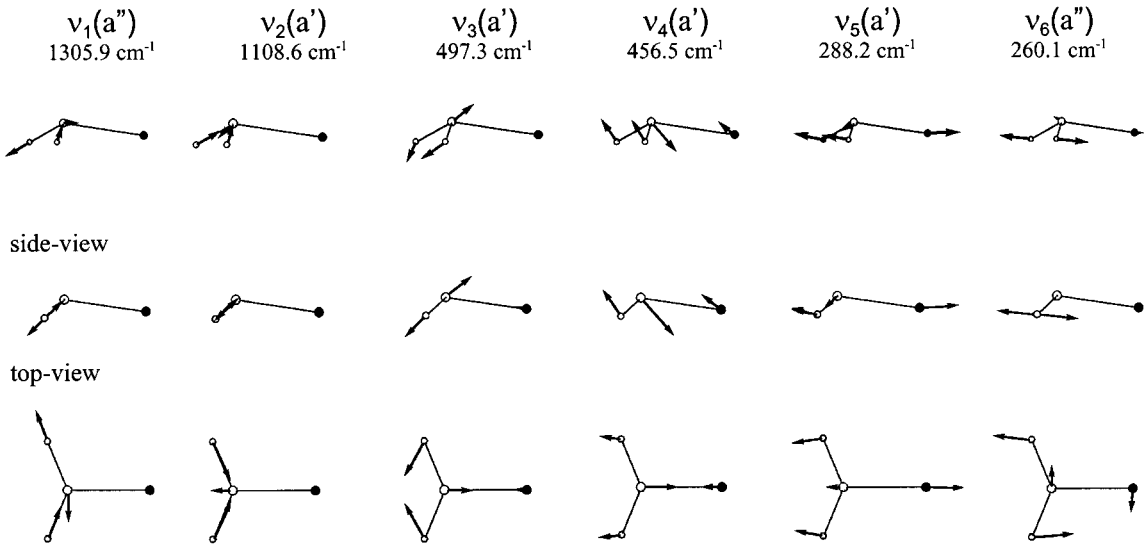

Figure 4. Displacement vector diagrams of vibrational modes of $ClSO_2$ calculated with the B3P86/aug-cc-pVTZ method. The modes are ordered by wavenumbers.

TABLE 4: Comparison of Observed Isotopic Ratios[a] of $ClSO_2$ with Predictions from Two Theoretical Methods

vib mode	species	B3LYP/ aug-cc-pVTZ	B3P86/ aug-cc-pVTZ	expt
ν_1	$^{35}Cl^{32}S(^{16}O)^{16}O$	(1273.4)[b]	(1305.9)[b]	(1309.5)[b]
	$^{37}Cl^{32}S(^{16}O)^{16}O$	1.0000	1.0000	1.0000
	$^{35}Cl^{34}S(^{16}O)^{16}O$	0.9871	0.9871	0.9863
	$^{35}Cl^{32}S(^{16}O)^{18}O$	0.9861	0.9860	0.9856
	$^{35}Cl^{32}S(^{18}O)^{18}O$	0.9681	0.9681	0.9680
ν_2	$^{35}Cl^{32}S(^{16}O)^{16}O$	(1085.5)	(1108.6)	(1098.5)
	$^{37}Cl^{32}S(^{16}O)^{16}O$	1.0000	1.0000	1.0000
	$^{35}Cl^{34}S(^{16}O)^{16}O$	0.9941	0.9941	0.9935
	$^{35}Cl^{32}S(^{16}O)^{18}O$	0.9750	0.9751	0.9755
	$^{35}Cl^{32}S(^{18}O)^{18}O$	0.9547	0.9547	0.9554
ν_3	$^{35}Cl^{32}S(^{16}O)^{16}O$	(488.6)	(497.3)	(497.0)
	$^{37}Cl^{32}S(^{16}O)^{16}O$	0.9993	0.9986	1.0000
	$^{35}Cl^{34}S(^{16}O)^{16}O$	0.9894	0.9883	0.9895
	$^{35}Cl^{32}S(^{16}O)^{18}O$	0.9825	0.9848	0.9835
	$^{35}Cl^{32}S(^{18}O)^{18}O$	0.9650	0.9702	0.9660
ν_4	$^{35}Cl^{32}S(^{16}O)^{16}O$	(434.7)	(456.5)	(454.2)/(455.3)[c]
	$^{37}Cl^{32}S(^{16}O)^{16}O$	0.9971	0.9972	−/0.9958
	$^{35}Cl^{34}S(^{16}O)^{16}O$	0.9807	0.9816	0.9811/0.9787
	$^{35}Cl^{32}S(^{16}O)^{18}O$	0.9931	0.9919	∼0.9963[d]/0.9936
	$^{35}Cl^{32}S(^{18}O)^{18}O$	0.9859	0.9827	0.9872/0.9848
ν_5	$^{35}Cl^{32}S(^{16}O)^{16}O$	(261.2)	(288.2)	
	$^{37}Cl^{32}S(^{16}O)^{16}O$	0.9849	0.9857	
	$^{35}Cl^{34}S(^{16}O)^{16}O$	0.9984	0.9988	
	$^{35}Cl^{32}S(^{16}O)^{18}O$	0.9918	0.9894	
	$^{35}Cl^{32}S(^{18}O)^{18}O$	0.9768	0.9748	
ν_6	$^{35}Cl^{32}S(^{16}O)^{16}O$	(248.5)	(260.1)	
	$^{37}Cl^{32}S(^{16}O)^{16}O$	0.9947	0.9947	
	$^{35}Cl^{34}S(^{16}O)^{16}O$	0.9957	0.9957	
	$^{35}Cl^{32}S(^{16}O)^{18}O$	0.9773	0.9789	
	$^{35}Cl^{32}S(^{18}O)^{18}O$	0.9619	0.9622	

[a] Ratios of ν(isotopomer)/$\nu(^{35}Cl^{32}S(^{16}O)^{16}O)$. [b] Calculated or observed $\nu(^{35}Cl^{32}S(^{16}O)^{16}O)$ in cm^{-1} are listed in parentheses. [c] Derived from deconvoluted lines; see text. [d] When the deconvoluted line at 455.3 cm^{-1} is used for $\nu(^{35}Cl^{32}S(^{16}O)^{16}O)$; see text.

wavelength, the Cl atom may have still greater excess energy after relaxation via collisions with matrix hosts to overcome the barrier. Excitation of SO_2 at 308 nm might lead to formation of the triplet state with lifetimes in the millisecond range; dissociation of Cl_2 and formation of triplet SO_2 in the same matrix cage might form Cl_2SO_2. The possibility that the absence of Cl_2SO_2 is due to secondary photolysis at 355 nm (rather than at 308 nm) is eliminated because the UV absorption spectrum of Cl_2SO_2 shows an absorption continuum beginning ∼360 nm and becoming increasingly intense toward smaller wavelengths. Secondary photolysis of $ClSO_2$ at 308, 355, 415, and 640 nm diminishes substantially the absorption of lines in set "a" with concomitant increase of SO_2 lines.

The small exothermicity (10−16 kcal mol^{-1}) of reaction 1 implies that its rate coefficient is small at room temperature because $ClSO_2$ decomposes readily to form Cl and SO_2. However, when one considers the equilibrium constant of the reaction, an equilibrium between Cl + SO_2 and $ClSO_2$ might be attained at a temperature less than 273 K. Hence, it is important to investigate both the gaseous reaction at low temperature and reactions of the adduct $ClSO_2$ with important species such as O_2, NO_2, and NO. Such information will help to assess the importance of reaction 1 in the atmosphere.

V. Conclusion

We have produced and identified $ClSO_2$ for the first time on irradiating at 355 nm a low-temperature matrix containing Cl_2 and SO_2. Lines at 1309.5, 1098.5, 497.0, and 454.2 cm^{-1} (or 1309.6, 1098.2, 497.7, and 455.8 cm^{-1}) are assigned to $ClSO_2$ isolated in solid Kr (or Ar) based on experiments with ^{34}S and ^{18}O isotopes and theoretical calculations. Present information indicates that Cl can react with SO_2 at low temperature to form $ClSO_2$, but not ClOSO. Further investigation of photochemistry and reactions of $ClSO_2$ is needed to assess the importance of the reaction Cl + SO_2 in the atmosphere.

Acknowledgment. The authors thank the National Science Council of the Republic of China (grant no. NSC89-2119-M-007-001) for support and the National Center for High-performance Computing for providing the facilities to perform part of the calculations.

Supporting Information Available: Predicted isotopic ratios for ^{34}S-, ^{18}O-, and ^{37}Cl-substituted isotopomers of two conformers of ClOSO and *cis*-ClSOO are listed in Table IS and IIS, respectively. This material is available free of change via the Internet at http://pubs.acs.org.

References and Notes

(1) Strattan, L. W.; Eibling, R. E.; Kaufman, M. *Atmos. Environ.* **1979**, *13*, 175.

(2) Eibling, R. E.; Kaufman, M. *Atmos. Environ.* **1983**, *17*, 429.

(3) Demore, W. B.; Yang, Y. L.; Smith, R. H.; Leu, M. T. *Icarus* **1985**, *63*, 347.
(4) Li, Z. *Chem. Phys. Lett.* **1997**, *269*, 128.
(5) Li, Z. *J. Phys. Chem. A.* **1997**, *101*, 9545.
(6) Kuo, Y.-P.; Wann, G. H.; Lee, Y.-P. *J. Chem. Phys.* **1993**, *99*, 3272.
(7) Lo, W.-J.; Lee, Y.-P. *J. Chem. Phys.* **1994**, *101*, 5494.
(8) Lo, W.-J.; Lee, Y.-P.; Tsai, J.-H. M.; Beckman, J. S. *Chem. Phys. Lett.* **1995**, *242*, 147.
(9) Lo, W.-J.; Shen, M.-y.; Yu, C.-h.; Lee, Y.-P. *J. Chem. Phys.* **1996**, *104*, 935.
(10) Jou, S.-H.; Shen, M.-y.; Yu, C.-h.; Lee, Y.-P. *J. Chem. Phys.* **1996**, *104*, 5745.
(11) Chen, L.-S.; Lee, C.-I.; Lee, Y.-P. *J. Chem. Phys.* **1996**, *105*, 9454.
(12) Lee, C.-I.; Lee, Y.-P.; Wang, X.; Qin, Q.-Z. *J. Chem. Phys.* **1998**, *109*, 10446.
(13) Bahou, M.; Lee, Y.-C.; Lee, Y.-P., submitted for publication in *J. Am. Chem. Soc.*
(14) *Gaussian 98* (Revision A.1); Frisch, M. J.; Trucks, G. W.; Schlegel, H. B.; Scuseria, G. E.; Robb, M. A.; Cheeseman, J. R.; Zakrzewski, V. G.; Montgomery, J. A.; Stratmann, R. E.; Burant, J. C.; Dapprich, S.; Millam, J. M.; Daniels, A. D.; Kudin, K. N.; Strain, M. C.; Farkas, O.; Tomasi, J.; Barone, V.; Cossi, M.; Cammi, R.; Mennucci, B.; Pomelli, C.; Adamo, C.; Clifford, S.; Ochterski, J.; Petersson, G. A.; Ayala, P. Y.; Cui, Q.; Morokuma, K.; Malick, D. K.; Rabuck, A. D.; Raghavachari, K.; Foresman, J. B.; Cioslowski, J.; Ortiz, J. V.; Stefanov, B. B.; Liu, G.; Liashenko, A.; Piskorz, P.; Komaromi, I.; Gomperts, R.; Martin, R. L.; Fox, D. J.; Keith, T.; Al-Laham, M. A.; Peng, C. Y.; Nanayakkara, A.; Gonzalez, C.; Challacombe, M.; Gill, P. M. W.; Johnson, B. G.; Chen, W.; Wong, M. W.; Andres, J. L.; Head-Gordon, M.; Replogle, E. S.; Pople, J. A. Gaussian Inc.: Pittsburgh, PA, 1998.
(15) Frisch, M.-J.; Head-Gordon, M.; Pople, J. A. *Chem. Phys. Lett.* **1990**, *166*, 275, 281.
(16) Becke, A. D. *J. Chem. Phys.* **1993**, *98*, 5648.
(17) Lee, C.; Yang, W.; Parr, R. G. *Phys. Rev.* **1988**, *B37*, 785.
(18) Becke, A. D. *Phys. Rev.* **1988**, *A38*, 3098.
(19) Perdew, J. P. *Phys. Rev.* **1986**, *B33*, 8822.
(20) Dunning, T. H. *J. Chem. Phys.* **1989**, *90*, 1007. Woon, D. E.; Dunning, T. H. Jr. *J. Chem. Phys.* **1993**, *98*, 1358.
(21) Kugel, R.; Taube, H. *J. Phys. Chem.* **1975**, *79*, 2130.
(22) Maillard, D.; Allavena, M.; Perchard, J. P. *Spectrochim. Acta* **1975**, *31A*, 1523.
(23) Suzuki, E. M.; Nibler, J. W.; Oakes, K. A.; Eggers, D. *J. Mol. Spectrosc.* **1975**, *58*, 201.
(24) Cheng, B.-M.; Lee, Y.-P. *J. Chem. Phys.* **1989**, *90*, 5930.
(25) Bondybey, V. E.; Fletcher, C. *J. Chem. Phys.* **1976**, *64*, 3615.
(26) Shimanouchi, T. *Tables of Molecular Vibrational Frequencies Consolidated Volume 1*; National Bureau of Standards: Washington, DC, 1972.
(27) McGrath, M. P.; Clemitshaw, K. C.; Rowland, F. S.; Hehre, W. J. *J. Phys. Chem.* **1990**, *94*, 6126.
(28) Birk, M.; Friedl, R. R.; Cohen, E. A.; Pickett, H. M.; Sander, S. P. *J. Chem. Phys.* **1989**, *91*, 6588.
(29) Matsumi, Y.; Tonokura, K.; Kawasaki, M. *J. Chem. Phys.* **1992**, *97*, 1065.
(30) McCaffrey, J. G.; Kunz, H.; Schwentner, N. *J. Chem. Phys.* **1992**, *96*, 155.